PERGAMON

International Journal of Solids and Structures 40 (2003) 763–776

INTERNATIONAL JOURNAL OF SOLIDS and STRUCTURES

www.elsevier.com/locate/ijsolstr

Interaction between a screw dislocation and viscoelastic interfaces

H. Fan *, G.F. Wang

School of Mechanical and Production Engineering, Nanyang Technological University, Singapore 639798, Republic of Singapore

Received 26 June 2002; received in revised form 12 September 2002

Abstract

The analytical solutions for the interaction between dislocations and interfaces are of great importance to materials scientists as well as to mechanics researchers. The interfaces are treated as perfectly bonded in the most of the existing research works, where the traction and displacement vectors are continuous across the interfaces. However, in reality, there are discontinuities of displacements across the interfaces. In the present paper, the interaction between a screw dislocation and an imperfect interface is considered. The imperfect interface is modeled by linear spring and dashpot, i.e. linearly elastic and viscoelastic behaviors are introduced to model the imperfection of the interface. Particularly, we solved the boundary value problem analytically for Kelvin and Maxwell type of interface. In terms of geometrical configurations, we obtained the solutions for two joint half-spaces and a circular inclusion embedded in an infinite matrix. The analytical results show that the force acting on the dislocation depends on the mismatch of materials and the imperfection of the interface and evolves as time elapses.

Keywords: Dislocation; Viscoelastic interface; Integral transforms

1. Introduction

The analytical research on the interaction between interfaces and dislocations started in early 1950s by Head (1953) who analyzed the force on a screw dislocation near an interface of a bi-material. Since then, dislocation interacting with interfaces has been an active research topic for solid mechanics researchers. The following two review articles give us a clear picture of the evolution of the research. Dundurs (1969) did the first detailed review, where he summarized most of the contributions up to the end of 1960s. Most recently, Chen (2001) reviewed the progress in the dislocation/interface interaction research in the past thirty years as part of his effort to study the dislocations interacting with wedged interfaces and inhomogeneities. Since the single dislocation interaction with interfaces can be considered as Green's function, there are a number of research topics derived from the dislocation/interface interaction research. The cracks (Griffith crack and

* Corresponding author.
E-mail address: mhfan@ntu.edu.sg (H. Fan).

0020-7683/02/$ - see front matter © 2002 Elsevier Science Ltd. All rights reserved.
PII: S0020-7683(02)00553-X

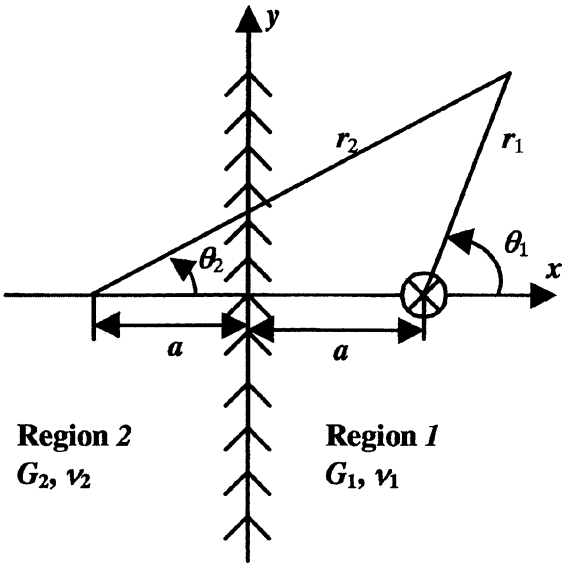

Fig. 1. A screw dislocation near an interface.

Zener–Stroh crack) have been formulated by using distributed dislocation concept (Weertman, 1996). The plasticity and strengthening phenomena have also been explained and calculated by dislocation mechanisms (Hirth and Lothe, 1982, and Mura, 1987).

It is noticed that in all the above mentioned research works, the interface was treated as perfectly bonded. In mechanics terminology, it is described by, referring to the configuration of Fig. 1,

$$\begin{aligned} &T_{\mathrm{i}}^{(2)}(0,y,t) = T_{\mathrm{i}}^{(1)}(0,y,t) \quad \text{traction continuity, and} \\ &u_{\mathrm{i}}^{(1)}(0,y,t) = u_{\mathrm{i}}^{(2)}(0,y,t) \quad \text{displacement continuity.} \end{aligned} \tag{1.1}$$

Introducing the imperfection to the interface gives us a useful analytical tool to model the damaged interface (Fan and Sze, 2001) and inter-phase (Hashin, 1991), to name a few. Among the various imperfect interface models, the linear spring model has been widely used and shown good agreements with the experimental data (Margetan et al., 1988; Lavrentyev and Rokhlin, 1998). The linear spring model also attracted attention from analytical researchers (for example, Zhong and Meguid (1997), Shilkrot and Srolovitz (1998) and Benveniste (1999)). As another imperfect interface model, the slipping model, in which interfaces have no resistance to the shear force, has also been adapted in many research works. Stagni and Lizzio (1992) investigated the dislocation in a lamella inhomogeneity with slipping interfaces. Chen et al. (1998) considered the dislocation near a sliding interface. More recently, Benveniste and Miloh (2001) made detailed classification of the imperfect interfaces by using an asymptotic expansion.

In the following sections, the interaction of a screw dislocation with viscoelastic interfaces is considered. The two materials adjacent to the interface are assumed to be linearly elastic, while the imperfect interface is assumed to be viscoelastic. Solutions for the Kelvin model and Maxwell model are derived for demonstration purpose. Two geometrical configurations are considered in Sections 2 and 3, i.e. two-joint infinitely extended half-spaces and a circular inhomogeneity embedded in an infinite matrix.

As a rule of thumb, the viscoelastic behavior should be considered when the working temperature of a solid is above 1/3 to 1/2 of its melting temperature (Kelvin scale). There are plenty of cases where the interface should be considered as viscoelastic. As an example, let us consider a case where two pieces of

metal (e.g. aluminum) are jointed by a lower melting temperature "glue" (e.g. epoxy). The melting temperature for aluminum is about 933 °K, while the melting temperature for epoxy is about 340–380 °K (Ashby and Jones, 1980). If this joint piece is working at room temperature (300 °K), the materials are considered as linear elastic, while the interface should be considered as viscoelastic.

2. A screw dislocation near viscoelastic interfaces

Firstly, let us consider a screw dislocation near an imperfect interface as depicted in Fig. 1. The Materials 1 and 2 adjacent to the interface are linearly elastic and their shear moduli are denoted by G_1 and G_2 (Poisson's ratios v_1, v_2 are not needed for anti-plane problem). The interface, on the other hand, possesses viscoelasticity. The coordinates are set up in such a way that the interface is along the y-axis and the screw dislocation is located in Material 1 at point $(a, 0)$.

For the present anti-plane configuration, the only non-vanishing displacement u_z is the function of coordinates x and y. Since the viscoelastic response comes from the interface, the inertia force can be neglected in Materials 1 and 2. Thus, the displacement u_z satisfies the Laplace's equation

$$\nabla^2 u_z = 0. \tag{2.1}$$

For a linearly elastic solid, the non-vanishing stress components are given by Hooke's law,

$$\sigma_{xz} = G\frac{\partial u_z}{\partial x}, \quad \text{and} \quad \sigma_{yz} = G\frac{\partial u_z}{\partial y}. \tag{2.2}$$

When $t = 0$, a screw dislocation is introduced into Material 1 and fixed at the position $(a, 0)$. For the sake of convenience, we take the plane $y = 0$ as the dislocation slipping plane, i.e.

$$\lim_{\eta \to 0}[u_z(x, -\eta, t) - u_z(x, \eta, t)] = b \quad (\text{for } \eta > 0, x > a \text{ and } t \geqslant 0), \tag{2.3}$$

where b is the magnitude of Burgers vector. At any moment, the traction across the interface is assumed to be continuous

$$\sigma_{xz}^{(2)}(0, y, t) = \sigma_{xz}^{(1)}(0, y, t), \tag{2.4}$$

where the superscripts "1" and "2" denote Materials 1 and 2. For the displacement condition on the interface, several models are available in the open literature, for example, the perfect interface (Head, 1953), the linear spring model (Hashin, 1991) and the slipping model (Chen et al., 1998). In the present study, we introduce the viscoelastic behavior to the imperfect interface.

Firstly let us consider the Kelvin model, in which a linear spring and a linear dashpot are parallel-connected (Shames and Cozzarelli, 1997). The relationship between the jump of displacement and the traction on the interface is given by

$$k[u_z^{(1)}(0, y, t) - u_z^{(2)}(0, y, t)] + \eta\frac{\partial}{\partial t}[u_z^{(1)}(0, y, t) - u_z^{(2)}(0, y, t)] = \sigma_{xz}^{(1)}(0, y, t), \tag{2.5}$$

where k is the "spring constant" of the interface and η is the viscosity coefficient.

At $t = 0$, when the dislocation is just introduced into Material 1, the displacement across the interface has no time to have a jump due to the dashpot. Therefore the initial condition for the displacement is read as

$$u_z^{(1)}(0, y, 0) = u_z^{(2)}(0, y, 0). \tag{2.6}$$

The solution to this boundary/initial value problem is assumed as

$$u_z^{(1)} = \frac{b}{2\pi}\underline{(\theta_1 + K\theta_2)} + \hat{u}_z^{(1)}, \tag{2.7}$$

$$u_z^{(2)} = \frac{b}{2\pi}\underline{[(1-K)\theta_1 + K\pi]} + \hat{u}_z^{(2)}, \tag{2.8}$$

where the definition of θ_1 and θ_2 are shown in Fig. 1 and

$$K = \frac{\Gamma - 1}{\Gamma + 1}, \quad \text{and} \quad \Gamma = G_2/G_1. \tag{2.9}$$

It is noticed that the underlined terms in Eqs. (2.7) and (2.8) are the solutions for the perfect interface (Dundurs, 1969), while the imperfection of the interface is included in $\hat{u}_z^{(1)}$ and $\hat{u}_z^{(2)}$ which are also harmonic functions, i.e.

$$\nabla^2 \hat{u}_z^{(1)} = 0, \quad \text{and} \quad \nabla^2 \hat{u}_z^{(2)} = 0. \tag{2.10}$$

To solve this boundary/initial value problem, we apply the Laplace's transformation to time t, and the Fourier transformation to the coordinate y. Thus, the displacement can be expressed as

$$\widehat{U}_z(x,s,p) = \int_0^\infty \int_{-\infty}^\infty \hat{u}_z(x,y,t) \mathrm{e}^{-\mathrm{i}sy} \mathrm{e}^{-pt}\, \mathbf{d}y\, \mathbf{d}t, \tag{2.11}$$

$$\hat{u}_z(x,y,t) = L^{-1}\left[\left(\frac{1}{2\pi}\int_{-\infty}^\infty \widehat{U}_z(x,s,p)\mathrm{e}^{\mathrm{i}sy}\,\mathrm{d}s\right), t\right], \tag{2.12}$$

where L^{-1} refers to the inverse formulae of Laplace's transformation. Substitution of Eq. (2.12) into Eq. (2.10) leads to

$$\left(\frac{\partial^2}{\partial x^2} - s^2\right)\widehat{U}_z(x,s,p) = 0. \tag{2.13}$$

Since the displacements should be finite as $x \to \infty$, we have the integral transformations of displacements in Materials 1 and 2 as

$$\widehat{U}_z^{(1)}(x,s,p) = A(s,p)\mathrm{e}^{-|s|(x-a)}, \tag{2.14}$$

$$\widehat{U}_z^{(2)}(x,s,p) = C(s,p)\mathrm{e}^{|s|(x+a)}. \tag{2.15}$$

By using the conditions of Eqs. (2.4), (2.5) and (2.6), $A(s)$ and $C(s)$ can be determined by

$$A(s,p) = -\Gamma C(s,p), \tag{2.16}$$

$$C(s,p) = \frac{\mathrm{i}}{2} b(K-1)\mathrm{sgn}(s)\frac{1}{p}\frac{a\mathrm{e}^{-2a|s|}}{|as| + \lambda + pt_0}, \tag{2.17}$$

where sgn(s) is the sign function

$$\mathrm{sgn}(s) = \begin{cases} 1 & s > 0 \\ 0 & s = 0 \\ -1 & s < 0 \end{cases}, \tag{2.18}$$

and

$$\lambda = ak\left(\frac{G_1 + G_2}{G_1 G_2}\right), \quad \text{and} \quad t_0 = a\eta\left(\frac{G_1 + G_2}{G_1 G_2}\right). \tag{2.19}$$

λ is a dimensionless parameter which measures the interface "rigidity" and t_0 is the relaxation time.

Substituting Eqs. (2.14)–(2.19) into (2.12), we can obtain the displacements $\hat{u}_z^{(1)}$ and $\hat{u}_z^{(2)}$ as

$$\hat{u}_z^{(1)}(x,y,t) = \frac{\Gamma b(K-1)}{2\pi}\int_0^\infty \frac{a\mathrm{e}^{-s(x+a)}}{as+\lambda}\left[1-\exp\left(-as\frac{t}{t_0}-\lambda\frac{t}{t_0}\right)\right]\sin(sy)\,\mathbf{d}s, \tag{2.20}$$

$$\hat{u}_z^{(2)}(x,y,t) = -\frac{b(K-1)}{2\pi}\int_0^\infty \frac{a\mathrm{e}^{s(x-a)}}{as+\lambda}\left[1-\exp\left(-as\frac{t}{t_0}-\lambda\frac{t}{t_0}\right)\right]\sin(sy)\,\mathbf{d}s. \tag{2.21}$$

Furthermore, substituting Eqs. (2.20) and (2.21) into Eqs. (2.7) and (2.8), and then using Hooke's law Eq. (2.2), we obtain the total stresses in the bi-materials as

$$\sigma_{zx}^{(1)}(x,y,t) = \frac{G_2 b(K-1)}{2\pi}\int_0^\infty \frac{\mathrm{e}^{-s(x+a)}}{as+\lambda}\left[\lambda+sa\exp\left(-as\frac{t}{t_0}-\lambda\frac{t}{t_0}\right)\right]\sin(sy)\,\mathbf{d}s - \frac{G_1 b}{2\pi}\left(\frac{y}{r_1^2}-\frac{y}{r_2^2}\right), \tag{2.22}$$

$$\sigma_{zy}^{(1)}(x,y,t) = -\frac{G_2 b(K-1)}{2\pi}\int_0^\infty \frac{\mathrm{e}^{-s(x+a)}}{as+\lambda}\left[\lambda+sa\exp\left(-as\frac{t}{t_0}-\lambda\frac{t}{t_0}\right)\right]\cos(sy)\,\mathbf{d}s + \frac{G_1 b}{2\pi}\left(\frac{x-a}{r_1^2}-\frac{x+a}{r_2^2}\right), \tag{2.23}$$

$$\sigma_{zx}^{(2)}(x,y,t) = \frac{G_2 b(K-1)}{2\pi}\int_0^\infty \frac{\mathrm{e}^{s(x-a)}}{as+\lambda}\left[\lambda+sa\exp\left(-as\frac{t}{t_0}-\lambda\frac{t}{t_0}\right)\right]\sin(sy)\,\mathbf{d}s, \tag{2.24}$$

$$\sigma_{zy}^{(2)}(x,y,t) = \frac{G_2 b(K-1)}{2\pi}\int_0^\infty \frac{\mathrm{e}^{s(x-a)}}{as+\lambda}\left[\lambda+sa\exp\left(-as\frac{t}{t_0}-\lambda\frac{t}{t_0}\right)\right]\cos(sy)\,\mathbf{d}s. \tag{2.25}$$

The elastic interaction energy for the configuration can be calculated by

$$E = \frac{1}{2}b\int_{a+r_0}^\infty \sigma_{zy}^{(1)}(x,0,t)\,\mathbf{d}x, \tag{2.26}$$

where r_0 is the radius of dislocation core, used to cancel the impropriety of elastic theory in the core. Using Eq. (2.23), we can obtain

$$E = \frac{b^2 G_1}{4\pi}\left\{\ln\left(\frac{2a}{r_0}\right)+\frac{2\Gamma}{\Gamma+1}\left[\mathrm{e}^{2\lambda}\mathbf{Ei}\left(2\lambda+\lambda\frac{t}{t_0}\right)+\int_0^\infty \frac{\mathrm{e}^{-2w}}{w+\lambda}\frac{\lambda}{w}\,\mathbf{d}w\right]\right\}, \tag{2.27}$$

where

$$\mathbf{Ei}(x) = \int_x^\infty \frac{\mathrm{e}^{-q}}{q}\,\mathbf{d}q, \text{ and } w = as. \tag{2.28}$$

The force acting on the dislocation is given by the negative gradient of the interaction energy with respect to the position of dislocation, a,

$$F = -\frac{\partial E}{\partial a} = -\frac{b^2 G_1}{4\pi a}\left[1-\frac{2\Gamma}{\Gamma+1}f_{\mathrm{K}}(\lambda,t/t_0)\right], \tag{2.29}$$

where

$$f_{\mathrm{K}}(\lambda,t/t_0) = 2\lambda\mathrm{e}^{2\lambda}\left[\mathbf{Ei}(2\lambda)-\mathbf{Ei}\left(2\lambda+\lambda\frac{t}{t_0}\right)\right]+\left(1+\frac{t}{2t_0}\right)^{-1}\exp\left(-\lambda\frac{t}{t_0}\right). \tag{2.30}$$

The subscript "K" refers to the Kelvin Model.

Fig. 2 shows the variation of $f_K(\lambda, t/t_0)$ with respect to t/t_0 for various λ. When λ tends to be infinity, $f_K = 1$, the force given by Eq. (2.29) tends to that for the perfect interface. When λ equals to zero, the interface is described by the dashpot only and evolves toward a free surface as time elapses. Fig. 3 shows the variation of $f_K(\lambda, t/t_0)$ with respect to λ for various t/t_0. It is seen that Γ and λ determine the initial and the final magnitude of the interacting force, while t_0 sets the process of the evolution.

Secondly, we apply Maxwell model to the interface. The constitutive Eq. (2.5) for the interface is replaced by

$$\frac{\partial}{\partial t}\left[u_z^{(1)}(0,y,t) - u_z^{(2)}(0,y,t)\right] = \frac{1}{k}\frac{\partial}{\partial t}\left[\sigma_{xz}^{(1)}(0,y,t)\right] + \frac{1}{\eta}\sigma_{xz}^{(1)}(0,y,t). \tag{2.31}$$

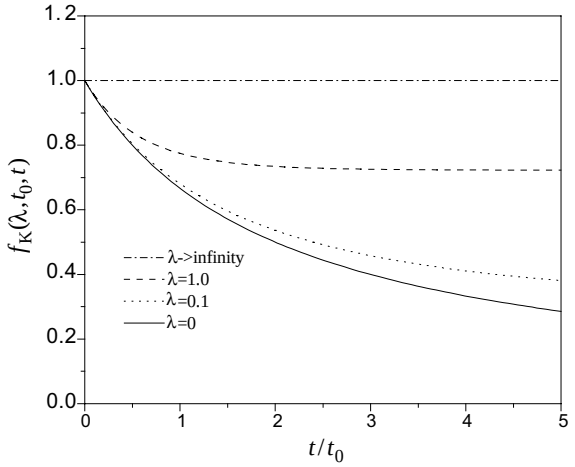

Fig. 2. The variation of $f_K(\lambda, t/t_0)$ vs. t/t_0.

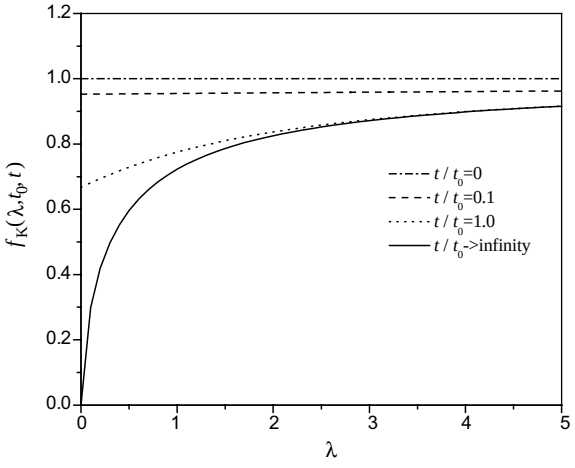

Fig. 3. The variation of $f_K(\lambda, t/t_0)$ vs. λ.

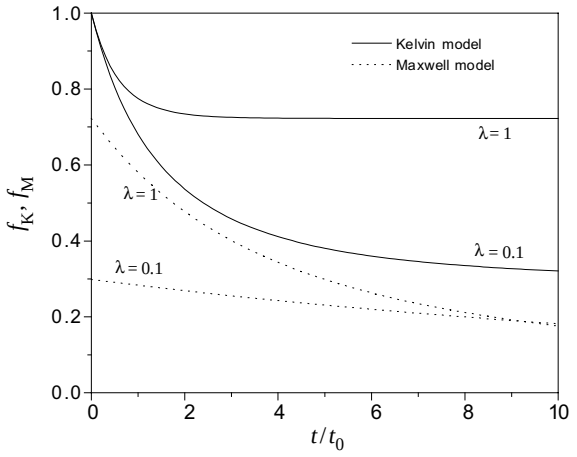

Fig. 4. Comparison between the Kelvin model and the Maxwell model.

At the moment of $t = 0$, the dashpot does not deform immediately, while the spring responds to the loading without time delay. Thus, the displacement across the interface exhibits an immediate jump as the response of the spring,

$$k[u_z^{(1)}(0,y,0) - u_z^{(2)}(0,y,0)] = \frac{G_2 b(K-1)}{2\pi} \int_0^\infty \frac{\lambda e^{s(x-a)}}{as+\lambda} \sin(sy)\,\mathbf{d}s. \tag{2.32}$$

Through a similar formulation, it is found that the interacting force on the screw dislocation takes the same form as Eq. (2.29), but f_K is replaced by

$$f_M(\lambda, t/t_0) = \int_0^\infty \frac{2\lambda e^{-2w}}{w+\lambda} \exp\left(-\frac{w\lambda}{w+\lambda}\frac{t}{t_0}\right)\mathbf{d}w, \tag{2.33}$$

where λ and t_0 are defined in Eq. (2.19) and the subscript "M" refers to the Maxwell model. It is noticed in Eq. (2.31) that the displacement jump increases till the traction on the interface reaches zero. In other words, the interface evolves toward a free surface when time elapses. The evolutions for Kelvin model and Maxwell model are compared in Fig. 4.

3. Discussion on special cases

In the above derivation, there are two interfacial parameters, namely, λ and t_0, defined in Eq. (2.19). The special cases, when these two parameters take limit values (zero and infinity), call for a detailed discussion.

Firstly, let us consider the Kelvin model governed by Eq. (2.5),

$$k[u_z^{(1)}(0,y,t) - u_z^{(2)}(0,y,t)] + \eta\frac{\partial}{\partial t}[u_z^{(1)}(0,y,t) - u_z^{(2)}(0,y,t)] = \sigma_{xz}^{(1)}(0,y,t). \tag{2.5}$$

(K1) $\boldsymbol{\eta} = \mathbf{0}$.

The vanishing coefficient of viscosity leads to a zero relaxation time, $t_0 = 0$. Eq. (2.5) becomes

$$k\lfloor u_z^{(1)}(0,y,t) - u_z^{(2)}(0,y,t)\rfloor = \sigma_{xz}^{(1)}(0,y,t). \tag{3.1}$$

The constitutive relation for the interface given by Eq. (3.1) is commonly called "linear spring model". It is realized that there is no time effect in the solution since the visco-effect vanishes. The force acting on the dislocation due to the imperfection of the interface is reflected by the curve of $t/t_0 \to \infty$ in Fig. 3.

(K2) $\boldsymbol{\eta \to \infty}$.

For this condition, (relaxation time $t_0 \to \infty$) and Eq. (2.5) becomes

$$\lfloor u_z^{(1)}(0,y,t) - u_z^{(2)}(0,y,t) \rfloor = F(y). \tag{3.2}$$

It refers to the prescribed displacement jump along the interface. One of the plausible physical models can be found in the dislocation theory of grain boundaries. The grain boundary was modeled as a pile up of dislocations or distributed dislocations along the grain boundary between two grains (Hirth and Lothe, 1982, Chapter 19). It should be pointed out that we need to relax the initial condition Eq. (2.6) $\lfloor u_z^{(1)}(0,y,0) - u_z^{(2)}(0,y,0) \rfloor = 0$ by Eq. (3.2) for the above physical phenomenon.

Nevertheless, our numerical result shown in Fig. 3 ($t/t_0 = 0$) for this limit converges to a perfect interface solution due to the initial condition Eq. (2.6).

(K3) $\boldsymbol{k = 0}$.

Eq. (2.5) is simplified as

$$\eta \frac{\partial}{\partial t}[u_z^{(1)}(0,y,t) - u_z^{(2)}(0,y,t)] = \sigma_{xz}^{(1)}(0,y,t), \tag{3.3}$$

that means the imperfect interface will deform like viscous fluid, which cannot resist the shear stress. Therefore, the jump of displacement does not stop increasing until the traction on the interface reaches zero, which means a free surface. The graphical result is shown in Fig. 2 by the curve $\lambda = 0$.

(K4) $\boldsymbol{k \to \infty}$.

This condition leads to

$$\lfloor u_z^{(1)}(0,y,t) - u_z^{(2)}(0,y,t) \rfloor = 0. \tag{3.4}$$

This is the condition for a perfect interface.

For the second viscoelastic model, Maxwell model, there are also four limit cases for our attention. The original constitutive equation for the interface is given by

$$\frac{\partial}{\partial t}[u_z^{(1)}(0,y,t) - u_z^{(2)}(0,y,t)] = \frac{1}{k}\frac{\partial}{\partial t}[\sigma_{xz}^{(1)}(0,y,t)] + \frac{1}{\eta}\sigma_{xz}^{(1)}(0,y,t). \tag{2.31}$$

(M1) $\boldsymbol{\eta = 0}$.

This condition corresponds to a zero relaxation time, $t_0 = 0$. Eq. (2.31) becomes

$$\sigma_{xz}^{(1)}(0,y,t) = 0. \tag{3.5}$$

This is the free surface condition. $f_{\mathrm{M}} = 0$ for this case.

(M2) $\boldsymbol{\eta \to \infty}$.

Under this condition, the interface is described by

$$k\lfloor u_z^{(1)}(0,y,t) - u_z^{(2)}(0,y,t) \rfloor = \sigma_{xz}^{(1)}(0,y,t). \tag{3.6}$$

It is the so-called linear spring model for the interface.

(M3) $\boldsymbol{k = 0}$.

Eq. (2.31) becomes

$$\sigma_{xz}^{(1)}(0,y,t) = H(y). \tag{3.7}$$

Table 1
Summary of the special cases

Interface model	$\eta = 0$	$\eta \to \infty$	$k = 0$	$k \to \infty$
Kelvin	Spring model	Prescribed jump of displacement	$\eta[\dot{u}] = \sigma$	Perfect interface
Maxwell	Free surface	Spring model	Free surface	$\eta[\dot{u}] = \sigma$

Our numerical solution converges to the free surface solution due to the constraint of the initial condition Eq. (2.32).

(M4) $k \to \infty$.

$$\eta \frac{\partial}{\partial t}[u_z^{(1)}(0,y,t) - u_z^{(2)}(0,y,t)] = \sigma_{xz}^{(1)}(0,y,t). \tag{3.8}$$

The interface is described by the dashpot only.

For the sake of quick reference, all the discussion in the present section is summarized in Table 1.

4. Screw dislocation interacting with circular inclusion

Let us consider a screw dislocation in the matrix as shown in Fig. 5, where $\xi > 1$. The Laplace's equation in the polar coordinate takes the form of

$$\nabla^2 u_z = \left(\frac{\partial^2}{\partial r^2} + \frac{\partial}{r\partial r} + \frac{\partial^2}{r^2 \partial^2 \theta} \right) u_z = 0. \tag{4.1}$$

Its general solution is assumed to be

$$u_z^{(1)} = \frac{b}{2\pi} \left\{ \underline{\theta_1 + K(\theta_2 - \theta)} + \sum_{n=1}^{\infty} \left(\frac{a}{r} \right)^n [a_n \cos(n\theta) + b_n \sin(n\theta)] \right\}, \tag{4.2}$$

$$u_z^{(2)} = \frac{b}{2\pi} \left\{ \underline{(1-K)\theta_1 + \pi K} + \sum_{n=1}^{\infty} \left(\frac{r}{a} \right)^n [c_n \cos(n\theta) + d_n \sin(n\theta)] \right\}, \tag{4.3}$$

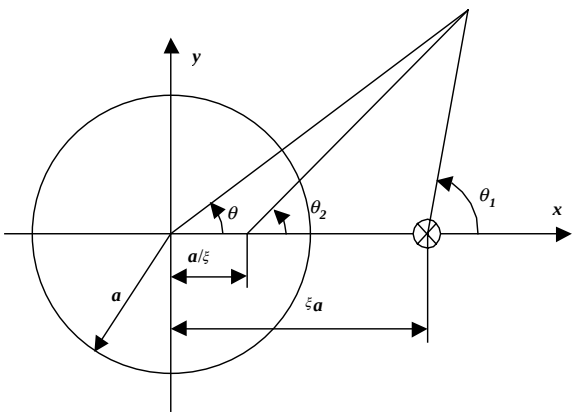

Fig. 5. A screw dislocation near a circular inclusion.

where $0 \leqslant \theta_1, \theta_2, \theta \leqslant 2\pi$ and K is defined by Eq. (2.9). Again, the underlined terms in Eqs. (4.2) and (4.3) are the solutions for the perfect interface (Dundurs, 1969). The effect of the imperfection of the interface is taken into account by the series solution.

The traction on the interface, $r = a$, is continuous

$$\sigma_{rz}^{(2)}(a,\theta) = \sigma_{rz}^{(1)}(a,\theta), \tag{4.4}$$

where

$$\sigma_{rz} = \sigma_{yz}\sin\theta + \sigma_{xz}\cos\theta. \tag{4.5}$$

The displacement condition on the imperfect interface is described by the Kelvin model. At the time $t = 0$,

$$u_z^{(1)}(a,\theta,0) - u_z^{(2)}(a,\theta,0) = 0. \tag{4.6}$$

When $t > 0$,

$$k[u_z^{(1)}(a,\theta,t) - u_z^{(2)}(a,\theta,t)] + \eta\frac{\partial}{\partial t}[u_z^{(1)}(a,\theta,t) - u_z^{(2)}(a,\theta,t)] = \sigma_{rz}^{(1)}(a,\theta,t). \tag{4.7}$$

Substituting Eqs. (4.2) and (4.3) into Eqs. (4.4) and (4.7) leads to

$$a_n = c_n = 0, b_n = -\Gamma d_n, \tag{4.8}$$

$$d_n = (1-K)\frac{T_K}{\pi}\int_{-\pi}^{\pi}\frac{\xi\sin\theta\sin(n\theta)}{1+\xi^2-2\xi\cos\theta}\,\mathbf{d}\theta, \tag{4.9}$$

$$T_K = \frac{1}{n+\lambda}\left[1-\exp\left(-\frac{\lambda+n}{t_0}t\right)\right], \tag{4.10}$$

where λ and t_0 are defined by Eq. (2.19). It should be pointed out that the parameter "a" in the present section is the radius of the circular inclusion, which is different from the "a" in Section 2.

The interaction energy of dislocation is given by

$$E = \frac{b^2G_1}{4\pi}\left[K\log\left(\frac{\xi^2}{\xi^2-1}\right) + \sum_{n=1}^{\infty}\Gamma(K-1)\frac{T_K}{\pi}\int_{-\pi}^{\pi}\frac{\xi^{1-n}\sin\theta\sin(n\theta)}{1+\xi^2-2\xi\cos\theta}\,\mathbf{d}\theta\right]. \tag{4.11}$$

The force acting on the dislocation is calculated by taking the derivative of E with respect to ξ (while a is a constant).

$$F_x = \underline{\frac{b^2G_1K}{2\pi a\xi(\xi^2-1)}}\left[1+\frac{\Gamma}{\Gamma-1}g_{1K}(\xi,\lambda,t/t_0)\right], \tag{4.12}$$

where

$$g_{1K} = \xi(\xi^2-1)\sum_{n=1}^{\infty}\left[\xi^{-n}\frac{T_K}{\pi}\int_{-\pi}^{\pi}\frac{1-n-(1+n)\xi^2+2n\xi\cos\theta}{(1+\xi^2-2\xi\cos\theta)^2}\sin\theta\sin(n\theta)\,\mathbf{d}\theta\right]. \tag{4.13}$$

If the Maxwell model is adopted on the interface,

$$\frac{\partial}{\partial t}[u_r^{(1)}(a,\theta,t) - u_r^{(2)}(a,\theta,t)] = \frac{1}{k}\frac{\partial\sigma_{rz}^{(1)}(a,\theta,t)}{\partial t} + \frac{1}{\eta}\sigma_{rz}^{(1)}(a,\theta,t). \tag{4.14}$$

The initial condition is

$$k[u_r^{(1)}(a,\theta,0)-u_r^{(2)}(a,\theta,0)]=\frac{bG_2(K-1)}{2\pi a}\sum_{n=1}^{\infty}\left[\frac{\lambda\sin(n\theta)}{n+\lambda}\frac{1}{\pi}\int_{-\pi}^{\pi}\frac{\xi\sin\theta'\sin(n\theta')}{1+\xi^2-2\xi\cos\theta'}\,\mathrm{d}\theta'\right]. \tag{4.15}$$

The corresponding results can be obtained by replacing Eq. (4.10) with

$$T_{\mathrm{M}}=\frac{1}{n+\lambda}+\frac{\lambda}{n+\lambda}\frac{1}{n}\left[1-\exp\left(-\frac{n\lambda}{n+\lambda}\frac{t}{t_0}\right)\right]. \tag{4.16}$$

As a counterpart problem of the above configuration, in the rest of this section, we will consider the case when the dislocation is inside the inclusion, $\xi<1$. The displacement field is structured as

$$u_z^{(1)}=\frac{b}{2\pi}\left[\underline{(1+K)\theta_1-K\theta}+\sum_{n=1}^{\infty}\left(\frac{a}{r}\right)^n(a_n\cos(n\theta)+b_n\sin(n\theta))\right], \tag{4.17}$$

$$u_z^{(2)}=\frac{b}{2\pi}\left[\underline{\theta_1+K(\pi-\theta_2)}+\sum_{n=1}^{\infty}\left(\frac{r}{a}\right)^n(c_n\cos(n\theta)+d_n\sin(n\theta))\right], \tag{4.18}$$

where a_n, b_n, c_n and d_n are given by Eqs. (4.8) and (4.9). $T(\lambda,t/t_0)$ takes the form of Eq. (4.10) for the Kelvin model and Eq. (4.16) for the Maxwell model.

The interaction energy of the dislocation is

$$E=\frac{b^2G_2}{4\pi}\left[K\log(1-\xi^2)-\frac{2}{\Gamma+1}\sum_{n=1}^{\infty}\frac{T}{\pi}\int_{-\pi}^{\pi}\frac{\xi^{n+1}\sin\theta\sin(n\theta)}{1+\xi^2-2\xi\cos\theta}\,\mathbf{d}\theta\right]. \tag{4.19}$$

The force acting on the dislocation is

$$F_x=\underline{\frac{b^2G_2K\xi}{2\pi a(1-\xi^2)}}\left[1+\frac{1}{\Gamma-1}g_2(\xi,\lambda,t/t_0)\right], \tag{4.20}$$

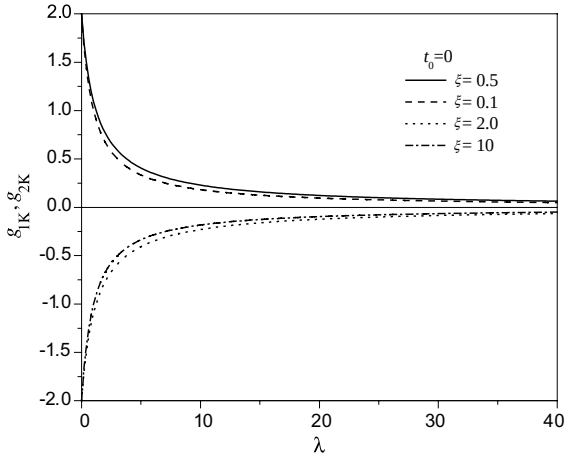

Fig. 6. The variation of g_{1K}, g_{2K} vs. λ.

where

$$g_2(\xi,\lambda,t/t_0)=\frac{1-\xi^2}{\xi}\sum_{n=1}^{\infty}\xi^n\frac{T}{\pi}\int_{-\pi}^{\pi}\frac{n+1+(n-1)\xi^2-2n\xi\cos\theta}{(1+\xi^2-2\xi\cos\theta)^2}\sin\theta\sin(n\theta)\,\mathrm{d}\theta. \tag{4.21}$$

Function g_1 and g_2 show weak dependence on ξ as shown in Fig. 6. It is also noticed that g_1 and g_2 depend on λ and t through the function $T(\lambda,t/t_0)$, therefore we only present the numerical results for g_1 as function of t and λ in Figs. 7 and 8 for the Kelvin model. Fig. 7 shows the variation of g_1 with respect to t/t_0 for various λ. When λ equals zero, the interface evolves toward a free surface as time elapses. Fig. 8 shows the variation of g_1 with respect to λ for various t/t_0 When the dislocation is just introduced into Material 1, there is no displacement jump across the interface. The results evolve toward that for the spring model as time elapses. A comparison is made between the Kelvin model and the Maxwell model in Fig. 9.

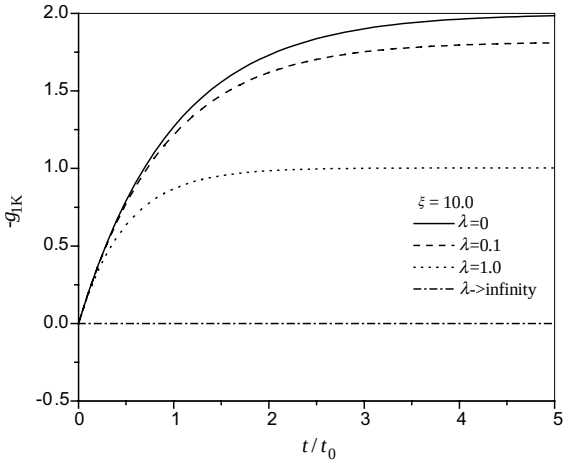

Fig. 7. Variation of g_{1K} vs. t/t_0.

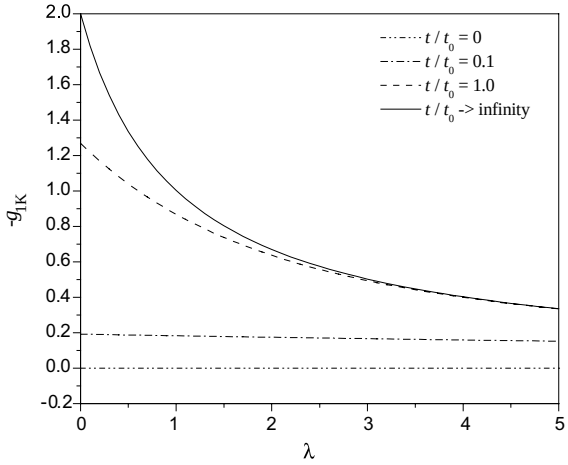

Fig. 8. The variation of g_{1K} vs. λ.

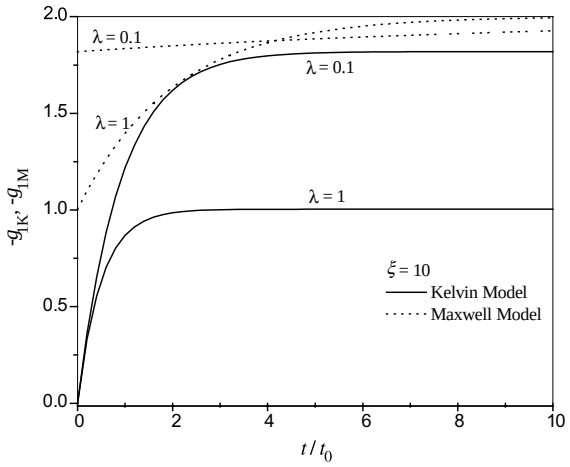

Fig. 9. Comparison of g_1 between the Kelvin model and the Maxwell model.

5. Concluding remarks

The analytical solutions for the interaction between a screw dislocation and an imperfect interface modeled by viscoelastic behavior are derived. The force acting on the dislocation depends on the modulus mismatch Γ, imperfection of the interface λ and normalized time t/t_0. The introduction of the dislocation in Material 1 at $t = 0$ gives the interface a so-called "creep" test loading. The evolution of the displacement jump across the interface depends on the viscoelastic models.

For the Kelvin model, the interacting force on dislocation starts with the value that a perfectly bonded interface exerts on the dislocation, then with the relaxation of the imperfect interface, and the force eventually reduces to the value for a spring modeled interface. The mismatch of the bi-materials and the imperfection of interface determine the initial and the final magnitude of the interacting force, while t_0 sets the process of evolution. For the Maxwell model, the interface evolves from the spring model towards a free surface. Solutions for other viscoelastic models with more constitutive parameters can also be obtained by using a similar derivation.

It should be pointed out that as the analytical solutions for both geometric configurations are presented in fairly simple forms, they can be applied as fundamental solutions for other research topics, such as dislocation pile ups, crack and composite mechanics.

Acknowledgements

The present research work was partially supported by the National Science and Technology Board of Singapore through the Center for Mechanics of Micro-System, School of Mechanical and Production Engineering, Nanyang Technological University, Singapore.

References

Ashby, M.F., Jones, D.R.H., 1980. Engineering Materials. Pergamon, Oxford, UK.

Benveniste, Y., 1999. On the decay of end effects in conduction phenomena: a sandwich trip with imperfect interfaces of low or high conductivity. J. Appl. Phys. 86 (3), 1273–1279.

Benveniste, Y., Miloh, T., 2001. Imperfect soft and stiff interface in two-dimensional elasticity. Mech. Mater. 33, 309–323.
Chen, B.J., 2001. Dislocation theory and its application in fracture analysis, Ph.D. thesis. School of Mechanical and Production Engineering, Nanyang Technological University, Singapore.
Chen, B.T., Hu, C.T., Lee, S., 1998. Dislocation near a sliding interface. Int. J. Eng. Sci. 36, 1011–1034.
Dundurs, J., 1969. Elastic interaction of dislocation with inhomogeneities. Mathematical Theory of Dislocations, ASME, New York, USA.
Fan, H., Sze, K.Y., 2001. A micro-mechanics model for imperfect interface in dielectric materials. Mech. Mater. 33, 363–370.
Hashin, Z., 1991. The spherical inclusion with imperfect interface. J. Appl. Mech. 58, 444–449.
Head, A.K., 1953. The interaction of dislocation and boundaries. Phil. Mag. 44, 92–94.
Hirth, J.P., Lothe, J., 1982. Theory of Dislocations, second ed. John-Willis, New York, USA.
Lavrentyev, A.I., Rokhlin, S.I., 1998. Ultrosonic spectroscopy of imperfect contact interfaces between a layer and two solids. J. Acoust. Soc. Am. 103 (2), 657–664.
Margetan, F.J., Thompson, R.B., Gray, T.A., 1988. Interfacial spring model for ultrosonic interactions with imperfect interfaces: theory of oblique incidence and application to diffusion-bonded butt joints. J. Nondestructive Eval. 7 (3/4), 131–152.
Mura, T., 1987. Micromechanics of Defects in Solids, second ed. Martinus Nijhoff Publisher, Dordrecht, Netherlands.
Shames, I.H., Cozzarelli, F.A., 1997. Elastic and Inelastic Stress Analysis. Taylor and Francis, London, UK.
Shilkrot, L.E., Srolovitz, D.J., 1998. Elastic analysis of finite stiffness bimaterial interfaces: application to dislocation-interface interactions. Acta Mater. 46 (9), 3063–3075.
Stagni, L., Lizzio, R., 1992. Interaction between an edge dislocation and a lamellar inhomogeneity with a slipping interface. J. Appl. Mech. 59, 215–217.
Weertman, J., 1996. Dislocation Based Fracture Mechanics. World Scientific Publisher, Singapore.
Zhong, Z., Meguid, S.A., 1997. On the elastic field of a spherical inhomogeneity with an imperfectly bonded interface. J. Elasticity 46, 91–113.